Synthesis and Characterization of Stable Cationic [Hydrotris(1-pyrazolyl)borato]Mo(CO)(NO)(η^3-allyl) Complexes—Solid-State and Solution Evidence for an η^2-Allyl Structure

Lawrence A. Villanueva, Yancey D. Ward,[1a] Rene Lachicotte, and Lanny S. Liebeskind*,[1b]

Sanford S. Atwood Chemistry Center, Emory University, 1515 Pierce Drive, Atlanta, Georgia 30322

Received January 23, 1996[⊗]

From the corresponding $TpMo(CO)_2(\pi\text{-allyl})$ complexes, four symmetrically substituted $TpMo(CO)(NO)(\pi\text{-allyl})^+$ complexes (π-allyl = propenyl, 2-methylpropenyl, cyclohexenyl, and cyclooctenyl) were prepared and characterized by IR, by ^1H and ^{13}C NMR spectroscopy, and in one case by X-ray crystallography. The BF_4^- salts of the cationic nitrosyl complexes were unstable in solution; however, using the noncoordinating counterion $[(3,5\text{-}(CF_3)_2C_6H_3)_4B]^-$ ($BAr'_4{}^-$) robust complexes were produced, permitting a thorough spectroscopic investigation. The crystal structure of $[TpMo(CO)(NO)(\eta^3\text{-}C_3H_5)][(3,5\text{-}(CF_3)_2C_6H_3)_4B]$ revealed a significant $\eta^3 \rightarrow \eta^2$ distortion of the allyl moiety. HETCOR and COSY NMR experiments were conducted in order to assign the chemical shifts of each of the allyl hydrogen and carbon atoms, unambiguously. These data also revealed the $\eta^3 \rightarrow \eta^2$ distortion of the allyl complexes. ^1H NOE experiments were carried out in order to determine the conformation of the allyl fragment for each nitrosyl complex. $[TpMo(CO)(NO)(\eta^3\text{-}C_3H_5)][BAr'_4]$ was formed as a mixture of *exo*/*endo* rotamers (5.2:1), while $[TpMo(CO)(NO)(\eta^3\text{-}C_4H_7)][BAr'_4]$ existed exclusively as the *endo* rotamer in solution. Only the *exo* rotamer was observed for the cyclic complexes $[TpMo(CO)(NO)(\eta^3\text{-}C_6H_9)][BAr'_4]$ and $[TpMo(CO)(NO)(\eta^3\text{-}C_8H_{13})][BAr'_4]$. A plausible mechanism for the formation of the cationic nitrosyl complexes involves the electrophilic addition of NO^+ to the neutral $TpMo(CO)_2(\eta^3\text{-allyl})$ complex with concurrent slippage of the allyl form η^3 to η^1 to generate a seven-coordinate cationic η^1-allyl complex. A deuterium labeling study using $TpMo(CO)_2(\eta^3\text{-}C_3H_4D)$ provided evidence for the $\eta^3 \rightarrow \eta^1$ mechanism responsible for the formation of *exo*/*endo* isomers.

Introduction and Background

The use of stoichiometric transition-metal π-allyl complexes for the regio- and stereocontrolled synthesis of organic molecules has garnered considerable attention in recent years. In particular, η^3-allyl and η^4-1,3-diene moieties coordinated to molybdenum have been thoroughly investigated.[2−34] One specific tactic for activating neutral $(\eta^5\text{-}C_5H_5)(\pi\text{-allyl})Mo(CO)_2$ species toward nucleophilic attack involves replacement of a CO ligand with NO^+, and this has led to considerable interest in the synthesis, characterization, and reactivity of $(\eta^5\text{-}C_5H_5)Mo(CO)(NO)(\pi\text{-allyl})^+$ complexes.[4,6−8,10,27,28,35−43]

In the late 1960s Trofimenko introduced the hydrotris(1-pyrazolyl)borate (Tp^-) ligand,[44] which can formally replace the η^5-cyclopentadienyl ligand in a very wide variety of systems.[45] Although a large number of $TpMo(CO)_2(\pi\text{-allyl})$ complexes have now been prepared and characterized,[46−48] there have been no literature reports of the corresponding cationic nitrosyl complexes. In order to understand the properties and reactivity of $TpMo(CO)(NO)(\pi\text{-allyl})^+$ complexes prior to their projected use in organic synthesis, their synthesis from

⊗ Abstract published in *Advance ACS Abstracts,* September 1, 1996.

(1) (a) Current address: Boehringer Ingelheim Pharm., Inc., 900 Ridgebury Road, P.O. Box 368, Ridgefield, CT 06877. (b) Telephone: (404) 727-6604. FAX: (404) 727-0845. E-mail: CHEMLL1@emory.edu.
(2) Faller, J. W.; Ma, Y. N. *Organometallics* **1993**, *12*, 1927.
(3) Faller, J. W.; Nguyen, J. T.; Ellis, W.; Mazzieri, M. R. *Organometallics* **1993**, *12*, 1434.
(4) Faller, J. W.; Lambert, C.; Mazzieri, M. R. *J. Organomet. Chem.* **1990**, *383*, 161.
(5) Faller, J. W.; Linebarrier, D. *Organometallics* **1988**, *7*, 1670.
(6) Faller, J. W.; Lambert, C. *Tetrahedron* **1985**, *41*, 5755.
(7) Faller, J. W.; Chao, K.-H. *Organometallics* **1984**, *3*, 927.
(8) Faller, J. W.; Chao, K. H.; Murray, H. H. *Organometallics* **1984**, *3*, 1231.
(9) Faller, J. W.; Murray, H. H.; White, D. L.; Chao, K. H. *Organometallics* **1983**, *2*, 400.
(10) Faller, J. W.; Chao, K.-H. *J. Am. Chem. Soc.* **1983**, *105*, 3893.
(11) Faller, J. W.; Rosan, A. M. *J. Am. Chem. Soc.* **1977**, *99*, 4858.
(12) Pearson, A. J.; Mallik, S.; Pinkerton, A. A.; Adams, J. P.; Zheng, S. *J. Org. Chem.* **1992**, *57*, 2910.
(13) Pearson, A. J.; Mallik, S.; Mortezaei, R.; Perry, M. W. D.; Shively, R. J., Jr.; Youngs, W. J. *J. Am. Chem. Soc.* **1990**, *1132*, 8034.
(14) Pearson, A. J.; Khetani, V. D. *J. Am. Chem. Soc.* **1989**, *111*, 6778.
(15) Pearson, A. J.; Blystone, S. L.; Nar, H.; Pinkerton, A. A.; Roden, B. A.; Yoon, J. *J. Am. Chem. Soc.* **1989**, *111*, 134.
(16) Pearson, A. J. In *Advances in Metal-Organic Chemistry*; Liebeskind, L. S., Ed.; JAI Press: Greenwich, CT, 1989; Vol. I, p 1.
(17) Pearson, A. J. *Philos. Trans. R. Soc. London, Ser. A* **1988**, *326*, 525.
(18) Pearson, A. J.; Khan, M. N. I.; Clardy, J. C.; He, C.-H. *J. Am. Chem. Soc.* **1985**, *107*, 2748.
(19) Pearson, A. J.; Khan, M. N. I. *J. Org. Chem.* **1985**, *50*, 5276.
(20) Pearson, A. J.; Khan, M. N. I. *J. Am. Chem. Soc.* **1984**, *106*, 1872.
(21) Pearson, A. J.; Khan, M. N. I. *Tetrahedron Lett.* **1984**, *25*, 3507.
(22) Yu, R. H.; McCallum, J. S.; Liebeskind, L. S. *Organometallics* **1994**, *13*, 1476.
(23) McCallum, J. S.; Sterbenz, J. T.; Liebeskind, L. S. *Organometallics* **1993**, *12*, 927.
(24) Rubio, A.; Liebeskind, L. S. *J. Am. Chem. Soc.* **1993**, *115*, 891.
(25) Liebeskind, L. S.; Bombrun, A. *J. Am. Chem. Soc.* **1991**, *113*, 8736.
(26) Hansson, S.; Miller, J. F.; Liebeskind, L. S. *J. Am. Chem. Soc.* **1990**, *112*, 9660.

S0276-7333(96)00041-6 CCC: $12.00

symmetrically substituted cyclic and acyclic $TpMo(CO)_2$-(π-allyl) moieties was undertaken and is reported herein. A detailed study of the diastereoselective synthesis and characterization of unsymmetrically substituted (π-allyl)molybdenum nitrosyl complexes based on the TpMo(CO)(NO) moiety has been completed and will be reported separately.

Results and Discussion

Preparation of $TpMo(CO)_2(\eta^3$-allyl) Complexes. Four symmetrically substituted (π-allyl)molybdenum complexes were chosen to assay the feasibility of CO → NO^+ conversion in the Tp (allyl)molybdenum system. Using a recently described method,[46] (π-allyl)molybdenum complexes **1**−**4** were prepared by the addition of the appropriate allylic bromide to a solution of $Mo(DMF)_3(CO)_3$[49] in CH_2Cl_2 followed by addition of K^+Tp^- (eq 1).

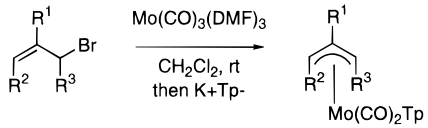

(1)

1: $R_1 = R_2 = R_3 = H$ 90%
2: $R_1 = Me$; $R_2 = R_3 = H$ 92%
3: $R_1 = H$; R_2-$R_3 = -(CH_2)_3-$ 45%
4: $R_1 = H$; R_2-$R_3 = -(CH_2)_5-$ 29%

By analogy with the related η^5-C_5H_5-based complexes, the allyl moiety can adopt either an *exo* or an *endo* conformation with respect to the $Mo(CO)_2$ unit (Figure 1). In the former the terminal carbon atoms of the allyl eclipse the CO ligands and the central carbon of the allyl eclipses the Mo. Rotation by 180° about the Mo−allyl centroid axis produces the *endo* conformer. ^1H NMR spectra of compounds **1**−**3**[47,48] and **4** displayed distinct, well-defined allyl signals which were attributed to the presence of only one conformer, rather than a rapidly interconverting mixture of *exo* and *endo* rotamers (see below). Compounds **1**[46] and **2**[50] exist as the *exo* rotamers in the solid state, and in a recent study it was pointed out that all $TpMo(CO)_2(\eta^3$-allyl) complexes that have been structurally characterized assume the *exo* conformation in the solid state as well as in solution.[46]

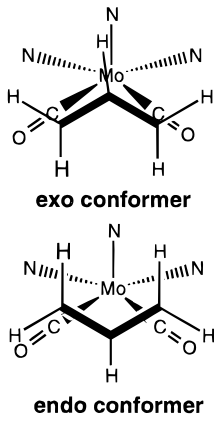

Figure 1.

Preparation of $[TpMo(CO)(NO)(\eta^3$-allyl)$][BF_4]$ Complexes. Polar, coordinating solvents such as acetonitrile and acetone are commonly used to generate $CpMo(CO)(NO)(\eta^3$-allyl$)^+$ complexes by CO → NO^+ exchange.[6−9,37,42,43,51] When solid $NOBF_4$ was added to solutions of **1**−**3** in acetonitrile at 0 °C, gas evolution and a sudden color change from yellow to deep orange-brown was observed. Evaporation of the acetonitrile and addition of diethyl ether to a CH_2Cl_2 solution of the residue at −60 °C induced precipitation of the nitrosyl complexes **5**−**7** in moderate to high yield (eq 2). Attempts to generate $[TpMo(CO)(NO)(\eta^3$-allyl$)][BF_4]$ complexes by the addition of 1−2 equiv of solid $NOBF_4$ to a solution of **1**−**3** in dimethoxyethane at −10 °C[52] resulted in incomplete conversion to the nitrosyl complex.

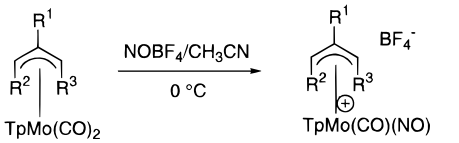

1-3

(2)

5: $R_1 = R_2 = R_3 = H$ 49%
6: $R_1 = Me$; $R_2 = R_3 = H$ 95%
7: $R_1 = H$; R_2-$R_3 = -(CH_2)_3-$ 80%

When stored under an inert atmosphere in the absence of light, compounds **5**−**7** were moderately stable in the solid state. However, in solution the instability of these nitrosyl complexes (bearing either BF_4^- or PF_6^- counterions) precluded complete spectroscopic characterization and the acquisition of satisfactory elemental analysis. One source of instability was traced to the tendency of these complexes to decarbonylate, possibly induced by fluoride ion formed on hydrolysis of BF_4^- or

(27) Lin, S.-H.; Chen, C.-C.; Vong, W.-J.; Liu, R.-S. *Organometallics* **1995**, *14*, 1619.
(28) Lin, S. H.; Lee, G. H.; Peng, S. M.; Liu, R. S. *Organometallics* **1993**, *12*, 2591.
(29) Su, G. M.; Lee, G. H.; Peng, S. M.; Liu, R. S. *J. Chem. Soc., Chem. Commun.* **1992**, 215.
(30) Lin, S. H.; Peng, S. M.; Liu, R. S. *J. Chem. Soc., Chem. Commun.* **1992**, 615.
(31) Yang, G. M.; Su, G. M.; Liu, R. S. *Organometallics* **1992**, *11*, 3444.
(32) Lin, S.-H.; Yang, Y.-J.; Liu, R.-S. *J. Chem. Soc., Chem. Commun.* **1991**, 1004.
(33) Yang, G.-M.; Lee, G.-H.; Peng, S.-M.; Liu, R.-S. *Organometallics* **1991**, *10*, 2531.
(34) Vong, W.-J.; Peng, S.-M.; Lin, S.-H.; Lin, W.-J.; Liu, R.-S. *J. Am. Chem. Soc.* **1991**, *113*, 573.
(35) McCleverty, J. A.; Murray, A. J. *Transition Met. Chem.* **1979**, *4*, 273.
(36) McCleverty, J. A.; Murray, A. J. *J. Chem. Soc., Dalton Trans.* **1979**, 1424.
(37) Faller, J. W.; Rosan, A. M. *J. Am. Chem. Soc.* **1976**, *98*, 3388.
(38) Bailey, N. A.; Kita, W. G.; McCleverty, J. A.; Murray, A. J.; Mann, B. E.; Walker, N. W. J. *J. Chem. Soc., Chem. Commun.* **1974**, 592.
(39) Faller, J. W.; Linebarrier, D. L. *Organometallics* **1990**, *9*, 3182.
(40) VanArsdale, W. E.; Winter, R. E. K.; Kochi, J. K. *Organometallics* **1986**, *5*, 645.
(41) Schilling, B. E. R.; Hoffmann, R.; Faller, J. W. *J. Am. Chem. Soc.* **1979**, *101*, 592.
(42) Adams, R. D.; Chodosh, D. F.; Faller, J. W.; Rosan, A. M. *J. Am. Chem. Soc.* **1979**, *101*, 2570.
(43) Faller, J. W.; Shvo, Y. *J. Am. Chem. Soc.* **1980**, *102*, 5396.
(44) Trofimenko, S. *J. Am. Chem. Soc.* **1967**, *89*, 3170.
(45) Trofimenko, S. *Chem. Rev.* **1993**, *93*, 943.
(46) Ward, Y. D.; Villlanueva, L. A.; Allred, G. D.; Payne, S. C.; Semones, M. A.; Liebeskind, L. S. *Organometallics* **1995**, *14*, 4132.
(47) Trofimenko, S. *J. Am. Chem. Soc.* **1969**, *91*, 588.
(48) Ipaktschi, J.; Hartmann, A. *J. Organomet. Chem.* **1992**, *431*, 303.
(49) Pasquali, M.; Leoni, P.; Sabatino, P.; Braga, D. *Gazz. Chim. Ital.* **1992**, *122*, 275.
(50) Holt, E. M.; Holt, S. L.; Watson, K. J. *J. Chem. Soc., Dalton Trans.* **1973**, 2444.
(51) Faller, J. W.; Shvo, Y.; Chao, K.; Murray, H. H. *J. Organomet. Chem.* **1982**, *226*, 251.
(52) Cosford, N. D. P.; Liebeskind, L. S. *Organometallics* **1994**, *13*, 1498.

PF_6^- in the presence of traces of water.[53,54] Although the addition of water to **5** and **7** afforded only intractable mixtures, the 2-methylpropenyl complex **6** reacted with H_2O in CD_2Cl_2 to yield 2-methyl-2-propen-1-ol and the aqua complex **8** (eq 3). Both the addition of water to

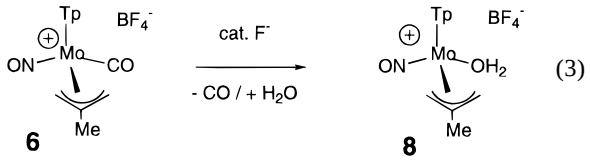

6 **8** (3)

(η^5-C_5H_5)(η^3-allyl)Mo(CO)(NO)$^+$ complexes to produce allylic alcohols[7,8] and the tendency of organometallic salts possessing BF_4^- as the counterion to generate aqua complexes have been reported.[55]

Evidence for the formation of the aqua complex **8** was found in the ^{1}H NMR spectrum, which showed the disappearance of the four allyl signals of **6**, the emergence of four new signals between 3.6 and 4.6 ppm, and the presence of new signals for the Tp ligand. The broad absorption at 6.25 ppm, which disappeared on D_2O exchange, was assigned to a coordinated H_2O ligand. In the IR spectrum of **8**, loss of a CO stretch at 2079 cm^{-1} and the appearance of an NO stretching absorption at 1688 cm^{-1} were consistent with the IR data reported for CpMo(H_2O)(NO)(η^3-C_7H_{13})$^+$ (ν_{NO} 1668 cm^{-1}).[56]

Preparation of [TpMo(CO)(NO)(η^3-allyl)][(3,5-(CF$_3$)$_2$C$_6$H$_3$)$_4$B] Complex. Because the instability of compounds **5**−**7** in solution prohibited their thorough spectroscopic investigation, stabilization of these reactive nitrosyl complexes was examined. Cationic organometallic salts possessing the noncoordinating counterion [(3,5-$(CF_3)_2C_6H_3)_4B]^-$ (BAr'_4^-) are significantly more stable than those with BF_4^- and PF_6^-.[57] Addition of solid $KBAr'_4$[57] to a CH_2Cl_2 solution of the cationic nitrosyl complexes generated *in situ* from **1**−**4** and $NOBF_4$ at 0 °C produced the nitrosyl complexes **9**−**12** in high yield after removal of CH_2Cl_2, dissolution of the residue in diethyl ether, filtration, and evaporation (eq 4). Compounds **9**−**12** are stable solids at room temper-

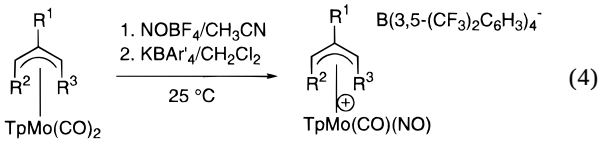

(4)

1-4

9: $R_1 = R_2 = R_3 = H$ 57%
10: $R_1 = Me$; $R_2 = R_3 = H$ 76%
11: $R_1 = H$; R_2-R_3 = -$(CH_2)_3$- 89%
12: $R_1 = H$; R_2-R_3 = -$(CH_2)_5$- 90%

ature and can be stored at 10 °C without any precautions. Furthermore, unlike the BF_4^- salts **5**−**7**, cationic complexes **9**−**12** were stable in solution at 25 °C for several days and showed no signs of decomposition or formation of the aqua complex, even in the presence of excess water. This observation provides strong support for the role of fluoride ion in the instability of **5**−**7** toward decarbonylation.

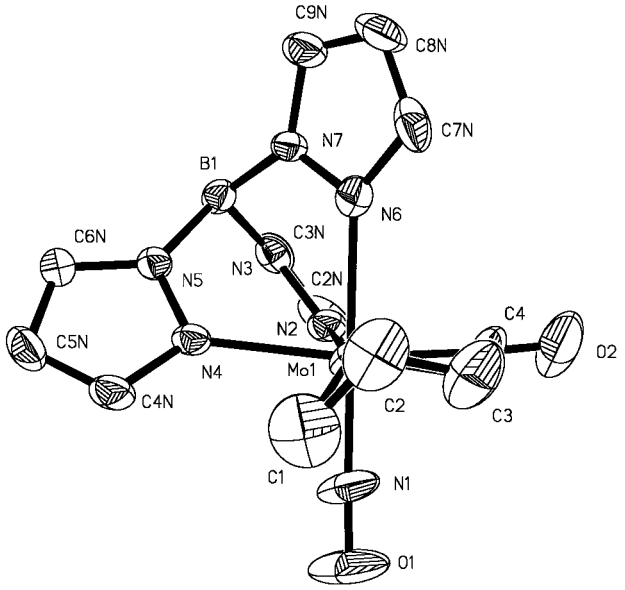

Figure 2.

Table 1. Selected Bond Lengths (Å) and Angles (deg) for [TpMo(CO)(NO)(η^3-C_3H_5)]-[(3,5-(CF$_3$)$_2$C$_6$H$_3$)$_4$B] (9)

Mo−C(1)	2.47(2)	Mo−N(4)	2.196(6)
Mo−C(2)	2.35(2)	Mo−N(6)	2.198(7)
Mo−C(3)	2.34(2)	O(2)−C(4)	1.161(11)
Mo−C(4)	2.011(10)	N(2)−C(1N)	1.314(14)
Mo−N(1)	1.833(9)	C(1)−C(2)	1.32(2)
Mo−N(2)	2.175(9)	C(2)−C(3)	1.43(2)

N(1)−Mo−N(6)	173.6(4)	C(4)−Mo−N(6)	87.8(4)
C(4)−Mo−N(4)	160.2(4)	N(2)−Mo−N(6)	83.0(3)
O(1)−N(1)−Mo	177.8(12)	N(1)−Mo−N(4)	95.3(3)
O(2)−C(4)−Mo	174.4(9)	O(1)−N(1)−Mo	177.8(12)
N(2)−Mo−C(2)	166.6(5)	O(2)−C(4)−Mo	174.4(9)
N(1)−Mo−C(4)	89.8(4)	C(1)−C(2)−C(3)	117(2)
N(1)−Mo−N(2)	90.8(4)		

Crystal Structure of [TpMo(CO)(NO)(η^3-C_3H_5)][(3,5-(CF$_3$)$_2$C$_6$H$_3$)$_4$B]. A crystal of **9** suitable for a diffraction study was grown from a CH_2Cl_2/hexane layer at 0 °C. A thermal ellipsoid plot of **9** is shown in Figure 2, with selected bond lengths and angles listed in Table 1. The structure of **9** clearly depicts the presence of the *exo* rotamer and reveals a significant $\eta^3 \rightarrow \eta^2$ distortion. The complex assumes a slightly distorted octahedral geometry with one pyrazole ligand and the NO group occupying axial sites, the N1−Mo−N6 angle of 173.6° best accommodating the greater π-accepting nature of the NO ligand compared to CO (N4−Mo−CO = 160.2°). The dissimilar π-accepting natures of the NO and CO ligands induce a twist in the η^3-allyl group, which brings two of the coordinated allyl carbon atoms (C(2) and C(3)) toward the equatorial plane of the distorted octahedral complex and nearly collinear with the Mo−CO axis, a phenomenon similar to that observed for CpMo(CO)(NO)(η^3-allyl)$^+$ complexes.[4,41] This geometry allows greater backbonding of Mo to the C(2)−C(3) unit with concomitant shortening of the Mo−C(2) and Mo−C(3) distances (2.35 and 2.34 Å, respectively) compared to Mo−C(1) (2.47 Å). Fully consistent with these distortions, the C(1)−C(2) bond distance (1.32 Å) is significantly shorter than C(2)−C(3) (1.43 Å) and suggests

(53) Jordan, R. F.; Dasher, W. E.; Echols, S. F. *J. Am. Chem. Soc.* **1986**, *108*, 1718.
(54) Reedijk, J. *Comments Inorg. Chem.* **1982**, *24*, 379.
(55) Beck, W.; Sünkel, K. *Chem. Rev.* **1988**, *88*, 1405.
(56) Linebarrier, D. L. Ph.D. Thesis, Yale University, 1989.
(57) Brookhart, M.; Grant, B.; Volpe, A. F. *Organometallics* **1992**, *11*, 3920.

Table 2. Chemical Shifts (ppm) and Coupling Constants (J_{H-H}, Hz) of the Allyl Carbons and Hydrogens of 9−12

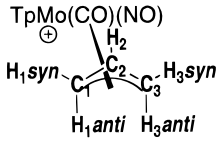

cmpd	C(1)	C(2)	C(3)	H(1)$_{syn}$	H(1)$_{anti}$	H(2)	H(3)$_{syn}$	H(3)$_{anti}$
9a	110.3	114.1	63.2	5.42, dd, ^3J = 7.3, ^4J = 3.4	5.28, d, ^3J = 14.7	5.49, m	4.60, ddd, ^3J = 7.4, ^2J and ^4J obscured	2.87, dd, ^3J = 12.5, ^2J = 3.0
9b	110.1	116.1	66.9	5.13, dd, ^3J = 7.3, ^4J = 3.0	4.41, d, ^3J = 14.6	5.99, m	4.60, obscured under H(3)$_{syn}$ of **9a**	3.15, dd, ^3J = 12.2, ^2J = 2.2
10	104.7	134.0	68.0	4.80, br d, ^4J = 4.0	4.12, d, ^2J = 1.5		4.39, dd, ^4J = 4.4, ^2J = 2.9	3.07, d, ^2J = 2.9
11	149.1	98.8	79.0	7.16, m		5.30, m	5.30, m	
12	147.5	106.7	83.1	6.75, app q, ^3J = 8.1		5.32, app t, ^3J = 8.1	5.24, app q, ^3J = 8.1	

almost complete double-bond character between C(1) and C(2) and a bond order between C(2) and C(3) near 1.5.

The ^{13}C and ^{1}H NMR data, reported below, are consistent with the $\eta^3 \rightarrow \eta^2$ distortions, indicating a similar structure in solution. The symmetrically substituted allyl complex [NMCpMo(CO)(NO)(η^3-C_3H_5)][BF_4] (NMCp = neomenthylcyclopentadienyl), though distorting to maximize back-bonding along the Mo−CO axis, did not reveal evidence of an $\eta^3 \rightarrow \eta^2$ allyl distortion in the solid state.[43] The strong tendency of Tp molybdenum complexes to achieve a six-coordinate octahedral geometry probably is responsible for the $\eta^3 \rightarrow \eta^2$ allyl distortions outlined above,[58] although nonbonding steric effects between the Tp ligand and the allyl moiety, which were deemed responsible for distortions in neutral TpMo(CO)$_2$(allyl) complexes,[46] may similarly contribute to the distortions in these cationic complexes.

Spectroscopic Characterization of [TpMo(CO)(NO)(η^3-allyl)][(3,5-(CF$_3$)$_2$C$_6$H$_3$)$_4$B] Complexes. Assignment of Resonances. HETCOR experiments were conducted on the two observed isomers of **9** and the single isomers of **10**−**12** in order to assign, unambiguously, ^{1}H and ^{13}C NMR resonances to individual π-allyl carbon atoms and to their attached hydrogen atom substituents (Table 2). Of the two different ^{13}C NMR absorptions originating from the terminal carbon atoms of the π-allyl ligands, it was assumed that the absorption of that carbon atom nominally *syn* to the NO ligand in both the *exo* and *endo* rotamers (C(1)) would appear downfield of the carbon atom nominally *syn* to the CO ligand (C(3)). This assumption followed from assignments made previously in the corresponding Cp-analog series,[52] and it was fully supported by all subsequent spectroscopic trends, described below. In each of the ^{13}C NMR spectra, C(1) appeared 40−50 ppm farther downfield than C(3). Furthermore, the ^{13}C NMR spectra of **9**−**12** show all C(1) *and* C(2) resonances downfield of the C(3) resonances, an observation that is consistent with a higher bond order for C(1)−C(2) than for C(2)−C(3). These data suggest a significant distortion of the allyl in solution, represented in the extreme as an $\eta^3 \rightarrow \eta^1$ allyl (C(1) → sp^2, C(3) → sp^3) or, perhaps more accurately, as $\eta^3 \rightarrow \eta^2$ allyl (C(1) → sp^2, C(3) → sp^3). This distortion complements that seen for **9-*exo*** in the solid state. It is of further interest that the chemical shift difference between C(1) and C(3) in the ^{13}C NMR spectra

(58) Curtis, M. D.; Shiu, K.-B. *Inorg. Chem.* **1985**, *24*, 1213.

Table 3. Difference in Chemical Shifts ($\Delta\delta$, ppm) between C(1) and C(3) for 9−12 and for the Analogous η^5-Cp-Based Complexes

cmpd	$\Delta\delta^{Tp}$(C(1)−C(3))	$\Delta\delta^{Cp}$(C(1)−C(3))[52]
9a	47.1	3.5
9b	43.2	8.1
10	36.7	5.2
11	70.1	9.5
12	64.4	n.a.

of **9**−**12** is considerably larger when compared to the difference between C(1) and C(3) of the analogous Cp complexes (Table 3),[52] an observation consistent with hapticity distortion in the Tp but not the Cp series.

The HETCOR spectral data, in consort with the observed ^{1}H NMR coupling constants (Table 2), allowed assignment of ^{1}H NMR absorptions to the specific *syn*, *anti*, and central hydrogen atoms of both isomers of **9** and to each allyl hydrogen atom of **10**−**12**. In the case of **9**, a 2D ^{1}H COSY spectrum was obtained in order to assign unambiguously the relative positions of the allyl signals in the ^{1}H NMR spectrum. The two hydrogen atoms attached to C(1) of the major isomer of **9** (**9a**) appeared as a 14.7 Hz double ($^3J_{1(anti)-2}$) at 5.28 ppm and a doublet of doublets ($^3J_{1(syn)-2}$ = 7.3 Hz, $^4J_{1(syn)-3(syn)}$ = 3.4 Hz) at 5.42 ppm. On the basis of the magnitude of these coupling constants, the former absorption was assigned to H(1)$_{anti}$ and the latter to H(1)$_{syn}$ (Table 2). The absence of observable coupling between the geminal pair of hydrogen atoms attached to C1 of **9** is consistent with the assignment of sp^2 hybridization to that carbon atom and to its very olefinic-like chemical shift in the ^{13}C NMR spectrum. The doublet of doublets at 2.87 ppm ($^3J_{3(anti)-2}$ = 12.5 Hz, $^2J_{3(anti)-3(syn)}$ = 3.0 Hz) was assigned to H(3)$_{anti}$, which possessed a small geminal coupling to H(3)$_{syn}$, and compared to H(1)$_{anti}$, it showed a smaller vicinal coupling to H(2). In contrast to the absence of an observable geminal coupling between H(1)$_{anti}$ and H(1)$_{syn}$, the appearance of a small geminal coupling between H(3)$_{anti}$ and H(3)$_{syn}$, the latter of which resonated at 4.60 ppm (overlapping ddd, $^3J_{3(syn)-2}$ = 7.4 Hz), is consistent with the drift of C3 toward sp^3 hybridization.

Using the same approach, all allyl protons of the minor isomer of **9** (**9b**) were assigned, except H(3)$_{syn}$, which was obscured by the absorption of H(3)$_{syn}$ of **9a** (Table 2). The doublet of doublets at 3.15 ppm ($^3J_{3(anti)-2}$ = 12.2 Hz, $^2J_{3(anti)-3(syn)}$ = 2.2 Hz) was attributed to H(3)$_{anti}$ and the doublet at 4.41 ppm ($^3J_{3(anti)-2}$ = 14.6 Hz) to H(1)$_{anti}$. The chemical shifts of C(1) and C(2),

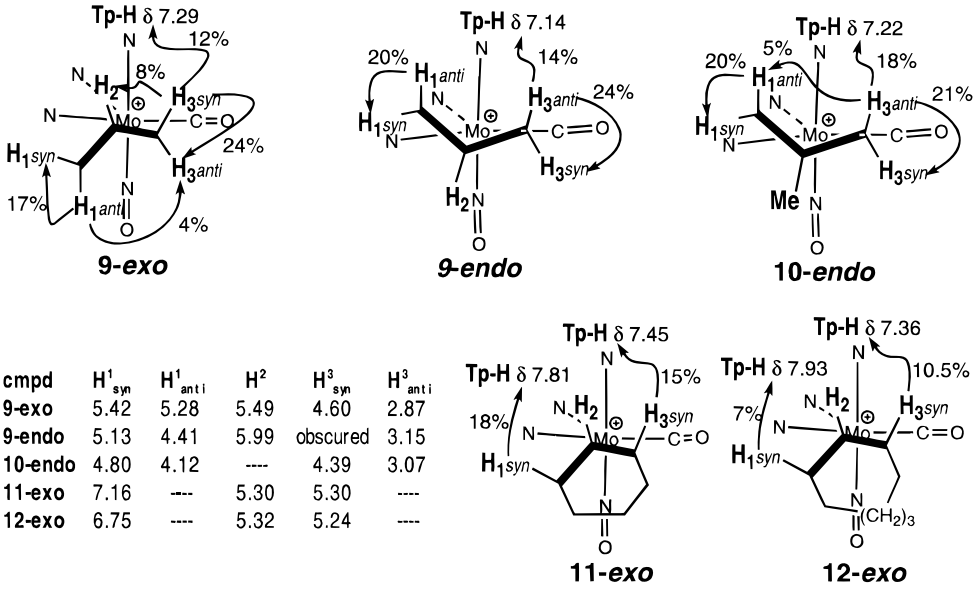

cmpd	H^1_{syn}	H^1_{anti}	H^2	H^3_{syn}	H^3_{anti}
9-exo	5.42	5.28	5.49	4.60	2.87
9-endo	5.13	4.41	5.99	obscured	3.15
10-endo	4.80	4.12	----	4.39	3.07
11-exo	7.16	----	5.30	5.30	----
12-exo	6.75	----	5.32	5.24	----

Figure 3.

and their attached hydrogen atoms, and the H−H coupling constants of **9b**, were consistent with the hybridization drift toward sp^2 at C(1) and toward sp^3 at C(3). The significant decrease in chemical shift of $H(1)_{anti}$ of **9b** relative to **9a** (4.41 ppm vs 5.42 ppm) is discussed below.

On the basis of the HETCOR spectrum of **10**, the hydrogen atom resonances appearing at 4.80 ppm (br d, $^4J_{1(syn)-3(syn)} = 4.0$ Hz) and at 4.12 ppm (d, $^2J_{1(anti)-1(syn)} = 1.5$ Hz) are attached to C(1) (δ 104.7), while the hydrogen atoms resonating at 4.39 ppm (dd, $^4J_{1(syn)-3(syn)} = 4.4$ Hz, $^2J_{3(anti)-3(syn)} = 2.9$ Hz) and at 3.07 ppm (d, $^2J_{3(anti)-3(syn)} = 2.9$ Hz) are bound to C(3) (δ 68.0) (Table 2). For the former pair of geminal hydrogens, the doublet at 4.12 ppm was assigned to $H(1)_{anti}$, because of the small observable geminal coupling, and the broad doublet at 4.80 was assigned to $H(1)_{syn}$ (long-range coupling to $H(3)_{syn}$). Accordingly, for the geminal pair of hydrogen atoms bound at C(3), the doublet at 3.07 ppm ($^2J = 2.9$ Hz) must be due to $H(3)_{anti}$ and the doublet of doublets at 4.39 ppm ($^4J_{3(anti)-1(syn)} = 4.4$ Hz, $^2J = 2.9$ Hz) to $H(3)_{syn}$. The assignment of the allyl signals was consistent with the NOE data presented below and with the assignments reported for the analogous η^5-cyclopentadienyl-based complex.[52]

In the cyclic allyl complexes **11** and **12**, H(1) and H(3) occupy *syn* positions, exclusively. HETCOR data for **12** revealed H(1) at 6.75 ppm attached to C(1) (at 147.5 ppm), and H(3) at 5.25 ppm bound to C(3) (83.1 ppm). The ^{1}H NMR spectrum of **12** displayed apparent quartets ($^3J = 8.1$ Hz) for H(1) and H(3), with H(2) appearing at 5.32 ppm as a triplet ($^3J = 8.1$ Hz). If we presume similar trends for the cyclohexenyl complex **11**, H(1) can be assigned to the multiplet at 7.16 ppm, while the resonances for both H(2) and H(3) overlap in a multiplet at 5.30 ppm. Compared to the acyclic complexes **9** and **10**, the chemical shift difference between C(1) and C(3) of **11** and **12** is significantly higher (Table 3), which suggests an even greater hapticity distortion (C(1) → sp^2, C(3) → sp^3) of the last two in solution.

Nuclear Overhauser Enhancement Experiments. ^{1}H NMR NOE experiments were conducted in order to determine the solution conformation of the allyl moiety of both isomers of **9** and of **10**−**12**. The ^{1}H NMR spectrum of **9** (as well as the BF_4^- analog **5**) revealed two sets of allyl signals, suggesting the presence of *exo* and *endo* rotamers (5.2:1) by analogy with the cyclopentadienyl system. The ^{13}C NMR spectrum also revealed two distinct sets of signals. However, attempted nuclear Overhauser enhancement experiments with complexes bearing the hydrotris(1-pyrazolyl)borato ligand were complicated by the broad B−H absorption in the ^{1}H NMR spectrum extending between 4 and 5 ppm. In order to perform unambiguous NOE experiments, the analogous B−D complex (Tp-*d*)Mo(CO)$_2$(η^3-C_3H_5) (**1-*d***) was prepared from Na(Tp-*d*). Generation of the nitrosyl complex under conditions identical with those described above afforded the nitrosyl complex **9-*d*** as a mixture of rotamers (6.0:1) whose ^{1}H NMR absorptions were assigned on the basis of the B−H analog data, described above. Presaturation of the multiplet at 4.60 ppm (overlapping *exo* and *endo* $H(3)_{syn}$) resulted in a 24% enhancement of the doublet of doublets at 2.87 ppm (*exo*-$H(3)_{anti}$), an 8% enhancement of the multiplet at 5.49 ppm (*exo*-H(2)), and a 12% enhancement of a Tp doublet at 7.29 ppm. Presaturation of the doublet at 5.28 ppm (*exo*-$H(1)_{anti}$) also produced a 4% enhancement of the doublet of doublets at 2.87 ppm (*exo*-$H(3)_{anti}$) and 17% enhancement of the doublet of doublets at 5.42 ppm (*exo*-$H(1)_{syn}$) (Figure 3). Attempts to presaturate the doublet of doublets at 5.42 ppm (*exo*-$H(1)_{syn}$) without irradiating the signal at 5.49 ppm (*exo*-H(2)) were unsuccessful. However, the 2D ^{1}H NOESY spectrum of **9** revealed an NOE cross-peak for $H(1)_{syn}$ and a Tp signal at 7.89 ppm. These NOE data are fully consistent with assignment of the *exo* conformation to the major rotamer (**9a**) in solution.

On the basis of the cyclopentadienyl analog resonances, it is reasonable to assign an *endo* conformation to the minor isomer **9b**, and ^{1}H NMR NOE experiments were consistent with that assignment (Figure 3). Of the two *anti* hydrogen substituents that should reside near the Tp ligand, only irradiation of the doublet of doublets at 3.15 ppm ($H(3)_{anti}$) produced an enhancement of Tp resonances (14% enhancement of the doublet appearing at δ 7.14). The absence of an NOE enhancement of any

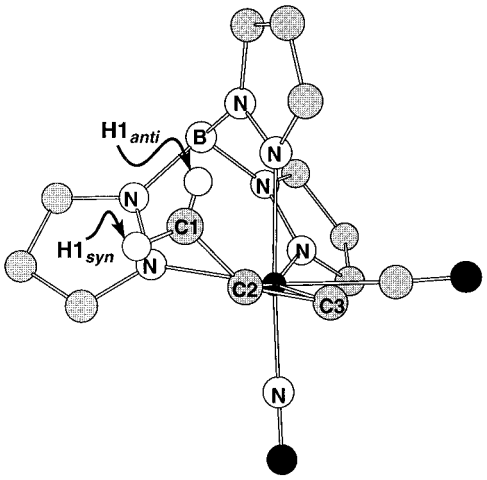

Figure 4.

of the Tp signals on presaturation of $H(1)_{anti}$ (δ 4.41) of **9-*endo*** is explained below. Consistent with the *endo* conformation, presaturation of $H(1)_{syn}$ (δ 5.13) did not result in enhancement of any Tp signals.

The ^{1}H NMR spectrum of **10** in $CDCl_3$ at 25 °C revealed the presence of only one rotamer whose conformation was established through NOE experiments (Figure 3). No enhancement of any of the Tp signals was seen on presaturation of the methyl signal at 2.29 ppm or of $H(1)_{syn}$ (δ 4.80) or $H(3)_{syn}$ (δ 4.39). However, presaturation of $H(3)_{anti}$ (δ 3.07) produced an 18% enhancement of one Tp signal (δ 7.22), a 21% enhancement of $H(3)_{syn}$ (δ 4.39 ppm), and 5% enhancement of $H(1)_{anti}$ (δ 4.12 ppm). These data suggest that compound **10** exists exclusively as the *endo* rotamer in solution. Presaturation of $H(1)_{anti}$ (δ 4.12) of **10**-*endo* did not result in enhancement of any of the Tp signals, a phenomenon that was also observed when $H(1)_{anti}$ of **9-*endo*** was presaturated, as indicated above.

Insight into the possible structures of **9-*endo*** and **10-*endo*** in solution can be deduced from the crystal structure of **9-*exo*** (Figure 2). Rotation about C(2)−C(3) of **9-*exo*** by 180° generates a view of **9-*endo*** that retains alignment of C(2)−C(3) along the Mo−CO bond axis (for maximum back-bonding) and places $H(1)_{anti}$ in the cleft generated by two of the pyrazole rings (Figure 4) *and not in proximity with any Tp ligand hydrogens*, a conformation consistent with the absence of Tp signal NOE enhancements when $H(1)_{anti}$ was irradiated. Furthermore, the chemical shift of $H(1)_{anti}$ of **9-*endo*** (δ 4.41) was significantly upfield relative to $H(1)_{anti}$ of **9-*exo*** (δ 5.28), which is consistent with the shielding of $H(1)_{anti}$ of **9-*endo*** by two of the pyrazole rings. Crystals of **10-*endo*** suitable for an X-ray diffraction study in order to confirm these observations could not be obtained. The exact nature of the *exo*/*endo* isomerization process is discussed below.

Consistent with earlier studies of η^5-CpMo(CO)(NO)(η^3-C_6H_9)$^+$,[52] ^{1}H NMR absorptions and ^{1}H NOE experiments were indicative of the formation of only the *exo* rotamer of the cyclohexenyl complex **11** (Figure 3). Irradiation of $H(1)_{syn}$ (δ, 7.16) produced an 18% enhancement of a Tp signal (δ 7.81), while irradiation of $H(3)_{syn}$ (δ 5.30) resulted in a 15% enhancement of a Tp signal at 7.45 ppm. Similar NOE results were observed for the cyclooctenyl analog **12**, which also displayed resonances for a single isomer in solution, assigned as the *exo* conformer. Irradiation of the apparent quartet at 6.76 ppm (C(1)−H) produced a 7% NOE enhancement of a Tp signal at 7.93 ppm (Figure 3). Likewise, irradiation of the apparent quartet at 5.24 ppm (C(3)−H) resulted in a 10.5% enhancement of a Tp signal at 7.36 ppm.

Investigation of the *exo*/*endo* Isomerism. In order to understand the formation of *endo* conformers from the acyclic allyl complexes, but not from the cyclic allyl complexes, a knowledge is required of both the mechanism of formation of the cationic nitrosyl complexes and the kinetic and thermodynamic parameters that influence their *exo*/*endo* interconversion. In a very limited way, the last two issues have been addressed. Variable-temperature NMR experiments on cationic nitrosyl complex **9** at 50 °C in $CDCl_3$ did not produce a change in the *exo*/*endo* ratio nor show evidence of coalescence of signals. Unfortunately, experiments above 60 °C resulted in decomposition. Nevertheless, the lack of exchange peaks between the allyl signals of the two rotamers in the 2D ^{1}H NOESY spectrum of **9** at 25 °C support the absence of *exo* and *endo* rotamer interconversion; similar experiments were used in a recent study to reveal an *exo*/*endo* isomerization process for a chiral palladium complex.[59]

In the cyclopentadienyl-based series, treatment of *exo*-CpMo(CO)$_2$(η^3-C_3H_5) with NO^+ gave *endo*-CpMo(CO)(NO)(η^3-C_3H_5)$^+$ as the kinetically formed product. Over time, the *endo* isomer equilibrated to the thermodynamically more stable *exo* product. Related results were observed on reaction of NO^+ with *endo*-CpMo(CO)$_2$(η^3-C_4H_7) (*exo* kinetic to *endo* thermodynamic) and *exo*-CpMo(CO)$_2$(η^3-cyclooctenyl) (*endo* kinetic to *exo* thermodynamic).[52] These observations directly contrast with the behavior of the Tp-based complexes investigated in this study—only the acyclic allyl complexes **9** and **10** formed any detectable *endo* conformer, and these did not isomerize to their corresponding *exo* conformers under the conditions explored.

The difference between the acyclic and cyclic allyl complexes can be attributed to (1) formation of *endo* rotamers in both series, but a significantly lower barrier to rotamer interconversion for the cyclic compared to the acyclic allyl complexes, and/or (2) a mechanistic basis for the appearance of *endo* conformers from the acyclic but not the cyclic complexes. At this time there are insufficient data to address *exo*/*endo* interconversions for the cyclic allyl complexes, but the *difference* between the acyclic and cyclic systems is strongly suggestive of the presence of an intermediate η^1-allyl complex, formed on addition of NO^+ to the TpMo(CO)$_2$(allyl) complex. If formed, the *acyclic* η^1-allyl complex can freely rotate about the allyl C(1)−C(2) bond; the *cyclic* η^1-allyl complexes cannot.

A plausible mechanistic rationale for the formation of cationic nitrosyl complexes from neutral TpMo(CO)$_2$(allyl) complexes is shown in Scheme 1, where electrophilic addition of NO^+ to the TpMo(CO)$_2$(allyl) complex occurs with concurrent slippage of the allyl from η^3 to η^1 and produces a seven-coordinate cationic η^1-allyl complex. Although for simplicity only pentagonal-bipyramidal seven-coordinate intermediates are depicted, the very low barrier to interconversion of seven-

(59) Breutel, C.; Pregosin, P. S.; Salzman, R.; Togni, A. *J. Am. Chem. Soc.* **1994**, *116*, 4067.

Scheme 1

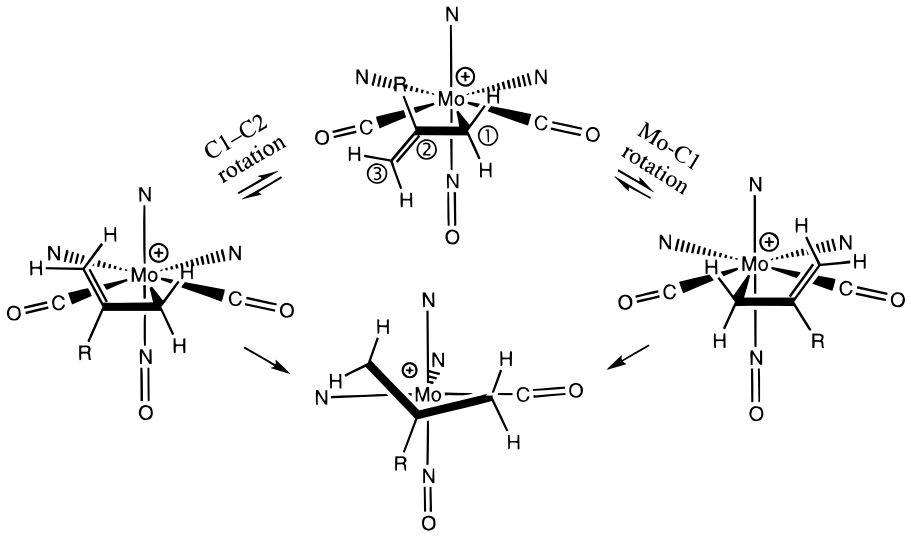

coordinate geometries and ligand environments in Tp−molybdenum complexes should render accessible alternate seven-coordinate geometries and produce no stereochemical barriers to placing a departing CO ligand cis to the η^1-allyl.[58] Loss of either CO ligand from a cationic seven-coordinate intermediate and re-formation of the η^3-allyl group can occur to produce either an *exo* or *endo* conformer. The *endo* conformers of the two *acyclic* η^1-allyl complexes can be produced by rotation about *either* C(1)−C(2) *or* Mo−C(1), but *only* Mo−C(1) rotation can convert the *cyclic* η^1-allyl complexes into their respective *endo* conformers.

Strong support for C(1)−C(2) rotation of the acyclic allyls leading to the *endo* conformer was obtained through a study of $TpMo(CO)_2(\eta^3\text{-}C_3H_4D)$ (Scheme 2). *syn*/*anti* isomerism of terminally substituted $TpMo(CO)_2$(allyl) complexes occurs by rotation about C(1)−C(2), a process that requires an η^1-allyl intermediate.[46] Therefore, if the *endo* conformer of the nitrosyl complex of the parent acyclic allyl complex is produced by rotation about C(1)−C(2) of an intermediate η^1-allyl, *syn*/*anti* isomerism of terminal substituents should occur in consort with *exo*/*endo* isomerism.

To test this hypothesis, treatment of $TpMo(CO)_2(\eta^3\text{-}C_3H_4D)$ (66% deuterium *anti*/34% deuterium *syn*)[46] with $NOBF_4/KBAr'_4$ produced a 6.7:1 mixture of *exo*/*endo* rotamers. Analysis of the product mixture by ^1H and ^2H NMR revealed each rotamer as a mixture of diastereomers (deuterium at either end of the allyl). For the *endo* rotamer, the ratio of the integral of resonances for all *anti* hydrogens to the allyl central hydrogen was 1.48:1, an increase from the 1.34:1 ratio observed for the dicarbonyl precursor $TpMo(CO)_2(\eta^3\text{-}C_3H_4D)$ (66% deuterium *anti*/34% deuterium *syn*). Assuming an equal population of the two possible η^1-allyl intermediates depicted in Scheme 2 (no deuterium isotope effect; deuterium at either terminus of the η^1-allyl), this degradation in the deuterium *anti* to *syn* ratio is close to the theoretical limit (1.5:1) that is calculated assuming that the *endo* rotamer is formed through a C(1)−C(2) rotation mechanism only. That is, *regardless* of the initial *anti*-D to *syn*-D ratio, beginning with one deuterium at an allyl terminus and formation of the *endo* product only by C(1)−C(2) rotation (through both of the equally probable η^1-allyls) will always produce an *anti*-H to central-H integral ratio of 1.5:1.0. On the other hand, if the *endo* product is formed by Mo−C(1) rotation only, the initial *anti*-D to *syn*-D ratio is unchanged in the product and the *anti*-H to central-H integral ratio will also be unchanged. In the case at hand, *endo* product formed exclusively through the Mo−C(1) rotation pathway would produce an *anti*-H to central-H integral ratio of 1.34:1.00. Therefore, inclusion of an *equally probable* Mo−C(1) rotation path to the *endo* rotamer would lower the observed integral ratio for the *anti* hydrogens to the allyl central hydrogen to 1.42:1. Unfortunately, overlapping resonances precluded a satisfactory analysis of the *syn* hydrogen/central hydrogen integral ratio for the *endo* rotamer.

Scheme 2

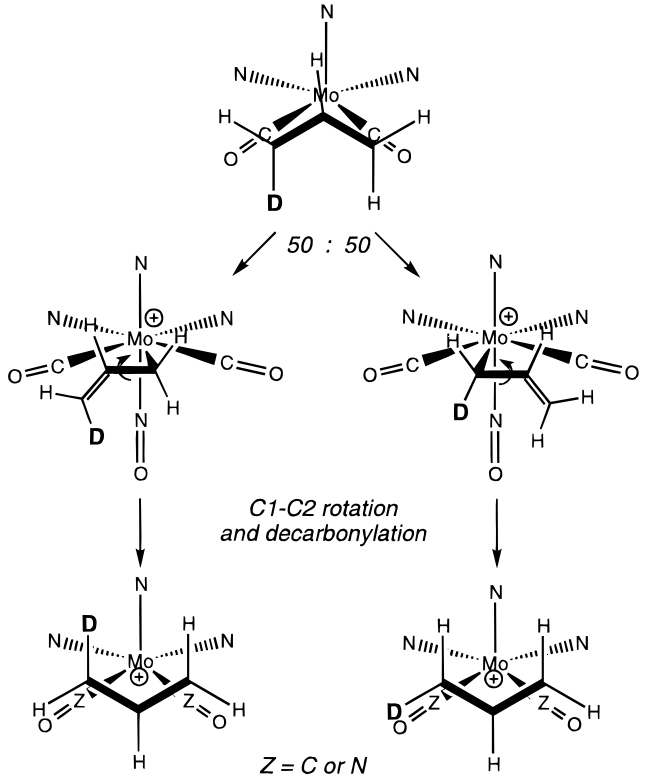

Three facts can be deduced from the study of the deuterated complex. First, the scrambling of deuterium both *syn*/*anti and* end to end are in accord with formation of the *endo* allyl nitrosyl cation through an η^1-allyl intermediate. Second, because the *anti*-H/central-H integral ratio is near 1.5:1, the *endo* rotamer must form almost exclusively through the C(1)−C(2) rotation mechanism. Finally, these data preclude the formation of the cationic *endo* nitrosyl complex by interception of a neutral η^3 *endo* dicarbonylmolybdenum complex (formed by rapid rotation about the Mo−allyl centroid axis of the dicarbonylmolybdenum allyl) with NO^+. This process, which does not occur, would retain the relative relationship between the substituent on the allyl central carbon and those in the *syn* and *anti* positions attached to the allyl terminal carbons.[37]

The absence of observable *endo* conformers from the two cyclic η^1-allyl complexes could be due to the significant nonbonded steric effects that must emerge as Mo−C(1) rotation brings the cyclic allyl into a geometry appropriate for *endo* η^3 bonding. At least for the two acyclic allyl complexes investigated in this study, the barriers leading to the transition states preceding formation of the *endo* conformers must be lower for C(1)−C(2) rotation than for Mo−C(1) rotation.

Conclusions

Four cationic TpMo(CO)(NO)(η^3-allyl) complexes were prepared by the addition of NO^+ to the corresponding neutral dicarbonyl compounds. The selection of counterion greatly influenced the overall stability of these complexes. The BF_4^- salts of the cationic nitrosyl complexes were unstable in solution and reacted readily with water; however, with $[(3,5\text{-}(CF_3)_2C_6H_3)_4B]^-$ as the counterion, the complexes exhibit high stability in solution and in the solid state.

The high stability of [TpMo(CO)(NO)(η^3-allyl)][(3,5-$(CF_3)_2C_6H_3)_4B$] complexes permitted their thorough spectroscopic characterization. ^1H and ^{13}C NMR data were consistent with distorted η^2-allyl structures for compounds **9**−**12** in solution, an analysis that was supported by the X-ray crystal structure of ***9-exo***. ^1H NOE experiments confirmed that **9** was formed as a mixture of *exo*/*endo* rotamers, while compounds **10**−**12** existed as only one rotamer in solution (**10**, *endo*; **11**, **12**, *exo*). Variable-temperature ^1H NMR experiments revealed a static, presumably kinetic conformer ratio for **9**. Data were presented to support the contention that the *exo*/*endo* ratio is established during the CO → NO^+ exchange process. In comparison to the formation of a mixture of *exo*/*endo* conformers of **9**, the exclusive generation of ***endo*-10** from ***exo*-2** suggests that steric effects play an important role in determining the *exo*/*endo* ratio.

Experimental Section

General Procedures. All procedures were carried out under an atmosphere of argon using standard Schlenk techniques. Acetonitrile, methylene chloride, and diethyl ether were dried with 4 Å molecular sieves, and the water content was analyzed using a Coulomatic Karl-Fischer titrimeter. Molybdenum hexacarbonyl, nitrosonium tetrafluoroborate, propargyl alcohol, $LiAlH_4$, allyl bromide, and 2-methallyl bromide were purchased from Aldrich Chemical Co. 3-Bromocyclohexene[60] and 3-bromocyclooctene[8] were prepared according to literature procedures. Potassium hydrotris(pyrazolyl)borate (KTp),[44] $Mo(DMF)_3(CO)_3$,[49] and $KBAr'_4$[57] were prepared using modified literature procedures. $TpMo(CO)_2(C_3H_4D)$ was prepared as described previously.[46] Na(Tp-*d*) was generated by the reaction between $NaBD_4$ (1 equiv) and pyrazole (4 equiv) at 200 °C using the procedure described for the synthesis of KTp.[44] Deuterated solvents were purchased from Cambridge Isotopes and dried over 4 Å sieves. All ^1H NOE experiments were performed on General Electric QE-360 or QE-500 spectrometers at 23 °C.

General Procedure for the Preparation of $TpMo(CO)_2(\eta^3$-allyl) Complexes. In a tared Schlenk tube under argon, $Mo(DMF)_3(CO)_3$ (1.0 equiv) was dissolved in 10−20 mL of dry, degassed CH_2Cl_2. The allyl bromide (1.1 equiv) in 1−2 mL of CH_2Cl_2 was then added at 25 °C. The solution was stirred at ambient temperature for 4−5 h; then, KTp (1.1 equiv) was added as a solid. After it was stirred for 1 h, the solution was filtered through a short plug of silica gel with CH_2Cl_2 as eluant to remove the precipitate. Removal of solvent by rotary evaporation afforded **1**−**4** as yellow solids. Purification was accomplished by flash SiO_2 chromatography with 1:4 EtOAc/hexane as eluant and recrystallization from CH_2Cl_2.

***exo*-$TpMo(CO)_2(\eta^3$-$C_3H_5)$ (1).** $Mo(DMF)_3(CO)_3$ (799 mg, 2.00 mmol), allyl bromide (266 mg, 2.20 mmol), and KTp (555 mg, 2.20 mmol) gave 732 mg (1.80 mmol) of product; 90% yield. Mp: 242−245 °C (lit.[47] 250−252 °C). ^1H NMR and IR data corresponded to those previously reported by Trofimenko[47] and Ipaktschi.[61] IR (CH_2Cl_2, KCl, cm^{-1}): 1944 (CO), 1851 (CO). ^1H NMR ($CDCl_3$, 300 MHz): δ 1.51 (d, J = 10.0 Hz, 2 H, C(1),C(3)−H_{anti}), 3.63 (d, J = 6.0 Hz, 2 H, C(1),C(3)−H_{syn}), 3.78 (m, 1 H, C(2)), 6.19 (br s, 3 H, Tp), 7.55 (br s, 3 H, Tp), 7.81 (br s, 2 H, Tp), 8.57 (br s, 1 H, Tp). ^{13}C NMR ($CDCl_3$, 75.5 MHz): δ 58.7 (C(1),C(3)), 73.9 (C(2)), 105.3 (br s, Tp), 135.8 (br s, Tp), 141.8 (br s, Tp), 227.5 (Mo−CO).

***exo*-$TpMo(CO)_2(\eta^3$-$C_4H_7)$ (2).** $Mo(DMF)_3(CO)_3$ (752 mg, 1.88 mmol), 2-methyl-3-bromopropene (280 mg, 2.07 mmol), and KTp (522 mg, 2.07 mmol) gave 728 mg (1.72 mmol) of product; 92% yield. Mp: 238-240 °C (lit.[62] 245−246 °C). IR (CH_2Cl_2, KCl, cm^{-1}): 1942 (CO), 1843 (CO). ^1H NMR ($CDCl_3$, 300 MHz): δ 1.38 (s, 2 H, C(1),C(3)−H_{anti}), 1.52 (s, 3 H, Me), 3.48 (s, 2 H, C(3)−H_{syn}), 6.20 (br s, 3 H, Tp), 7.54 (br s, 3 H, Tp), 7.99 (br s, 3 H, Tp). ^{13}C NMR ($CDCl_3$, 75.5 MHz): δ 18.4 (Me), 58.9 (C(1),C(3)), 83.4 (C(2)), 105.3 (br s, Tp), 135.6 (br s, Tp), 142.4 (br s, Tp), 227.1 (Mo−CO).

***exo*-$TpMo(CO)_2(\eta^3$-$C_6H_9)$ (3).** $Mo(DMF)_3(CO)_3$ (685 mg, 1.72 mmol) 3-bromocyclohexene (337 mg, 2.06 mmol), and KTp (477 mg, 1.89 mmol) gave 341 mg (0.76 mmol) of product; 45% yield. Mp: 295−297 °C (lit.[47] 300−302 °C). Spectroscopic data corresponded to those previously reported by Trofimenko[47] and Ipaktschi.[61] IR (CH_2Cl_2, KCl, cm^{-1}): 1934 (CO), 1845 (CO). ^1H NMR ($CDCl_3$, 300 MHz): δ 0.43 (m, 1 H, CH_2), 1.09 (m, 1 H, CH_2), 1.55 (br s, 1 H, CH_2), 2.10 (m, 3 H, CH_2), 3.71 (t, J = 7.0 Hz, 1 H, C(2)), 4.29 (br d, J = 5.0 Hz, 2 H, C(1),C(3)-H), 6.16 (app t, J = 2.0 Hz, 2 H, Tp), 6.29 (app t, J = 2.0 Hz, 1 H, Tp), 7.50 (d, J = 2.0 Hz, 1 H, Tp), 7.56 (d, J = 2.0 Hz, 2 H, Tp), 7.75 (d, J = 2.0 Hz, 2 H, Tp), 8.60 (d, J = 2.0 Hz, 1 H, Tp). ^{13}C NMR ($CDCl_3$, 75.5 MHz): δ 19.4 (CH_2), 23.2 (CH_2), 67.8 (C(2)), 71.9 (C(1),C(3)), 105.1 (Tp), 105.8 (Tp), 134.2 (Tp), 135.8 (Tp), 141.6 (Tp), 147.2 (Tp), 226.6 (Mo−CO).

***exo*-$TpMo(CO)_2(\eta^3$-$C_8H_{13})$ (4).** $Mo(DMF)_3(CO)_3$ (3.11 g, 7.79 mmol), 3-bromocyclooctene (1.77 g, 9.35 mmol), and KTp (2.36 mg, 9.34 mmol) gave 1.07 g (2.26 mmol) of product; 29% yield. Mp: 210 °C dec. (CH_2Cl_2/hexane, 1:4). IR (CH_2Cl_2, KCl, cm^{-1}): 1933 (CO), 1840 (CO). ^1H NMR ($CDCl_3$, 300 MHz): δ 1.60 (m, 7 H), 2.27 (m, 1 H), 2.62 (m, 2 H), 4.03 (app t, J = 8.3 Hz, 1 H), 4.37 (app q, J = 8.8 Hz, 2 H), 6.16 (app t, J = 2.2 Hz, 2 H), 6.26 (app t, J = 2.2 Hz, 1 H), 7.47 (d, J = 2.2 Hz, 1

(60) Dauben, H. J.; McCoy, L. L. *J. Am. Chem. Soc.* **1959**, *81*, 4863.
(61) Ipaktschi, J.; Hartmann, A.; Boese, R. *J. Organomet. Chem.* **1992**, *434*, 303.
(62) Trofimenko, S. *J. Am. Chem. Soc.* **1969**, *91*, 3183.

H), 7.54 (d, $J = 2.2$ Hz, 2 H), 7.83 (d, $J = 1.7$ Hz, 2 H), 8.57 (d, $J = 2.2$ Hz, 1 H). ^{13}C NMR ($CDCl_3$, 75.5 MHz): δ 230.1 (CO), 147.4 (Tp), 142.1 (Tp), 135.7 (Tp), 134.1 (Tp), 105.7 (Tp), 105.2 (Tp), 80.5 (C(2)), 75.2 (C(1),C(3)), 33.5 (CH_2), 28.5 (CH_2), 23.6 (CH_2). Anal. Calcd for $C_{19}H_{23}BN_6O_2Mo$: C, 48.13; H, 4.89; N, 17.71. Found: C, 48.24; H, 4.93; N, 17.55.

General Procedure for the Preparation of [TpMo(η^3-allyl)(CO)(NO)][BF_4] Complexes. The $TpMo(CO)_2(\eta^3$-allyl) complex was dissolved in dry, degassed acetonitrile and stirred under an atmosphere of argon at 0 °C. Nitrosonium tetrafluoroborate (1.4 equiv) was added as a solid (CO evolution), and stirring was continued for 30 min at 0 °C. Removal of solvent under reduced pressure gave the cationic molybdenum nitrosyl complex, which was purified by precipitation from CH_2Cl_2 at −60 °C using diethyl ether. All nitrosyl complexes were stable in the solid state and were stored under an inert atmosphere in the absence of light. The sensitivity of complexes **5**−**7** in solution prevented the acquisition of satisfactory analytical data.

[TpMo(CO)(NO)(η^3-C_3H_5)][BF_4] (5). *exo*-$TpMo(CO)_2(\eta^3$-C_3H_5) (304 mg, 0.75 mmol, 1.0 equiv) and $NOBF_4$ (135 mg, 1.16 mmol, 1.54 equiv) gave 184 mg (0.37 mmol) of a light yellow solid product; 7.9:1 mixture of *exo* and *endo* conformers, 49% yield. Mp: 95−97 °C dec. IR (CH_2Cl_2, KCl, cm^{-1}): 2101 (CO), 1734 (NO). *exo* ^{1}H NMR (CD_2Cl_2, 300 MHz): δ 3.31 (dd, $J = 13.0$, 3.0 Hz, 1 H, C(3)−H_{anti}), 5.08 (dd, $J = 7.0$, 2.0 Hz, 1 H, C(3)−H_{syn}), 5.57 (m, 2 H, C(1)−$H_{syn,anti}$), 5.63 (m, 1 H, C(2)−H), 6.36 (app t, $J = 2.0$ Hz, 1 H, Tp), 6.47 (app t, $J = 2.0$ Hz, 1 H, Tp), 6.51 (app t, $J = 2.0$ Hz, 1 H, Tp), 7.68 (d, $J = 2.0$ Hz, 1 H, Tp), 7.87 (d, $J = 2.0$ Hz, 1 H, Tp), 7.91 (d, $J = 2.0$ Hz, 1 H, Tp), 7.93 (d, $J = 2.0$ Hz, 1 H, Tp), 8.22 (d, $J = 2.0$ Hz, 1 H, Tp), 8.39 (d, $J = 2.0$ Hz, 1 H, Tp). *endo* ^{1}H NMR (CD_2Cl_2, 300 MHz): 3.49 (d, $J = 11.8$ Hz, 1H, C(3)−H_{anti}), 4.50 (m, C(3)−H_{syn}, 1H), 5.00 (m, 1H, C(1)−H_{anti}), 5.28 (m, 1H, C(1)−H_{syn}), 6.41 (app t, $J = 2.2$ Hz, 1H, Tp), 6.50 (app t, $J = 2.2$ Hz, 1H, Tp), 7.56 (d, $J = 1.5$ Hz, 1H, Tp), 7.90 (d, $J = 1.4$ Hz, 1H, Tp), 7.92 (d, $J = 3.0$ Hz, 1H, Tp), 7.93 (d, $J = 3.0$ Hz, 1H, Tp). *exo* ^{13}C NMR (CD_2Cl_2, 75.5 MHz): δ 65.9 (C3)), 107.4 (Tp), 107.6 (Tp), 108.0 (Tp), 109.9 (C(1)), 115.2 (C2)), 137.3 (Tp), 138.4 (Tp), 143.0 (Tp), 145.6 (Tp), 147.1 (Tp), 203.6 (Mo−CO).

***endo*-[TpMo(CO)(NO)(η^3-C_4H_7)][BF_4] (6).** *exo*-TpMo-$(CO)_2(\eta^3$-C_4H_7) (2.00 g, 4.76 mmol, 1.0 equiv) and $NOBF_4$ (612 mg, 5.24 mmol, 1.1 equiv) gave 2.35 g (4.62 mmol) of an olive green solid product; 95% yield. Mp: 86−89 °C dec. IR (CH_2Cl_2, KCl, cm^{-1}): 2112 (CO), 2067, 2010, 1728 (NO). ^{1}H NMR ($(CD_3)_2CO$, 300 MHz): δ 2.53 (s, 3 H, Me), 3.76 (d, $J = 2.0$ Hz, 1 H, C(3)−H_{anti}), 4.34 (br s, 1 H, C(1)−H_{anti}), 5.21 (dd, $J = 4.0$, 2.0 Hz, 1 H C(3)−H_{syn}), 5.29 (d, $J = 4.0$ Hz, 1 H, C(1)−H_{syn}), 6.42 (app t, $J = 2.0$ Hz, 1 H, Tp), 6.48 (app t, $J = 2.0$ Hz, 1 H, Tp), 6.60 (app t, $J = 2.0$ Hz, 1 H, Tp), 7.98 (d, $J = 2.0$ Hz, 1 H, Tp), 8.16 (d, $J = 2.0$ Hz, 1 H, Tp), 8.20 (d, $J = 3.0$ Hz, 1 H, Tp), 8.23 (d, $J = 3.0$ Hz, 1 H, Tp), 8.35 (d, $J = 2.0$ Hz, 1 H, Tp), 8.47 (d, $J = 2.0$ Hz, 1 H, Tp). ^{13}C NMR (CD_2Cl_2, 75.5 MHz): δ 22.7 (Me), 70.3 (C(3)), 104.4 (C(1)), 107.5 (Tp), 107.8 (Tp), 134.5 (C2)), 137.9 (Tp), 138.2 (Tp), 138.7 (Tp), 143.4 (Tp), 144.6 (Tp), 146.2 (Tp), 202.1 (Mo−CO).

***exo*-[TpMo(CO)(NO)(η^3-C_6H_9)][BF_4] (7).** *exo*-$TpMo(CO)_2$-$(\eta^3$-C_6H_9) (669 mg, 1.50 mmol, 1.0 equiv) and $NOBF_4$ (228 mg, 1.95 mmol, 1.3 equiv) gave 643 mg (1.20 mmol) of a yellow solid product; 80% yield. Mp: 90 °C dec. IR (CH_2Cl_2, KCl, cm^{-1}): 2079 (CO), 1722 (NO). ^{1}H NMR (CD_2Cl_2, 300 MHz): δ 1.38 (m, 1 H, CH_2), 1.59 (m, 1 H, CH_2), 2.45 (m, 1 H, CH_2), 3.17 (m, 3 H, CH_2), 5.37 (t, $J = 8.0$ Hz, 1 H, C(2)−H), 5.66 (m, 1 H, C(3)−H), 6.38 (app t, $J = 2.0$ Hz, 1 H, Tp), 6.45 (app t, $J = 2.0$ Hz, 1 H, Tp), 6.49 (app t, $J = 2.0$ Hz, 1 H, Tp), 7.35 (m, 1 H, C(1)−H), 7.67 (d, $J = 2.0$ Hz, 1 H, Tp), 7.79 (br s, 2 H, Tp), 7.83 (d, $J = 2.0$ Hz, 1 H, Tp), 8.00 (d, $J = 2.0$ Hz, 1 H, Tp), 8.21 (d, $J = 2.0$ Hz, 1 H, Tp). ^{13}C NMR (CD_2Cl_2, 75.5 MHz): δ 17.6 (CH_2), 25.4 (CH_2), 26.5 (CH_2), 80.7 (C(3)), 98.9 (C(2)), 107.5 (Tp), 107.7 (Tp), 136.9 (Tp), 138.2 (Tp), 138.3 (Tp), 142.3 (Tp), 145.4 (Tp), 146.3 (Tp), 148.6 (Tp), 150.7 (C(1)), 207.0 (Mo−CO).

Addition of Water to [TpMo(CO)(NO)(η^3-C_4H_7)][BF_4] (6). Procedure A. In a Schlenk tube, **6** (138, 0.26 mmol) was dissolved in 10 mL of CH_2Cl_2. Via syringe, 5 equiv of H_2O (or D_2O) was added, and the solution was stirred at ambient temperature for 24 h. Solvent was removed under reduced pressure, affording **8** as a brown solid. IR (CH_2Cl_2, KCl, cm^{-1}): 1945, 1850, 1688 (NO). ^{1}H NMR (CD_2Cl_2, 300 MHz): δ 2.49 (s, 3 H, Me), 3.56 (br d, $J = 4.4$ Hz, 1 H), 3.61 (d, $J = 2.2$ Hz, 1 H), 4.03 (s, 1 H), 4.48 (d, $J = 3.7$ Hz, 1 H), 6.25 (br s, 2 H, H_2O), 6.38 (m, 3 H, Tp), 7.50 (d, $J = 1.5$ Hz, 1 H, Tp), 7.76 (m, 2 H, Tp), 7.87 (d, $J = 3.0$ Hz, 1 H, Tp), 7.89 (d, $J = 3.0$ Hz, 1 H, Tp), 7.96 (d, $J = 2.0$ Hz, 1 H, Tp). ^{13}C NMR (CD_2Cl_2, 75.5 MHz): δ 22.5 (Me), 87.4 (C(3)), 94.9 (C(1)), 106.8 (Tp), 106.9 (Tp), 107.6 (Tp), 135.8 (Tp), 137.0 (C(2)), 137.7 (Tp), 138.5 (Tp), 142.4 (Tp), 142.5 (Tp), 146.1 (Tp).

Procedure B. In an NMR tube, 15 mg of **6** was dissolved in 0.5 mL of CD_2Cl_2. Water was added via syringe (2−3 equiv), and the reaction was monitored by ^{1}H NMR spectroscopy. After 1 h at 25 °C, the ^{1}H NMR spectrum revealed the presence of the aqua complex **8** as well as 2-methyl-2-propen-1-ol.

General Procedure for the Preparation of [TpMo(CO)(NO)(η^3-allyl)][(3,5-$(CF_3)_2C_6H_3)_4B$] Complexes. Procedure A. [TpMo(CO)(NO)(η^3-allyl)][BF_4] was dissolved in 15 mL of CH_2Cl_2 under argon at 25 °C. To this solution, solid $KBAr'_4$ (1 equiv) was added at 25 °C. After the mixture was stirred for 30 min, the solution color was dark yellow and cloudy. Solvent was removed under reduced pressure, and the yellow-brown residue was extracted with diethyl ether (20 mL). The yellow-orange solution was filtered via cannula and the solvent removed under reduced pressure to yield the nitrosyl complexes as orange-brown solids. Recrystallization in CH_2Cl_2/hexane at 0 °C gave yellow crystals of analytical purity.

Procedure B. A solution of $TpMo(CO)_2(\eta^3$-allyl) was dissolved in 10−20 mL of CH_2Cl_2, and the solution was cooled to 0 °C in an ice bath. Solid $NOBF_4$ was slowly added, and the solution was stirred for 30 min at 0 °C. Solid $KBAr'_4$ was added, and the solution was stirred for an additional 30 min. Using the identical workup described in procedure A afforded the corresponding nitrosyl complex.

[TpMo(CO)(NO)(η^3-C_3H_5)][(3,5-$(CF_3)_2C_6H_3)_4B$] (9). *exo*-$TpMo(CO)_2(\eta^3$-C_3H_5) (204 mg, 0.50 mmol, 1.0 equiv), $NOBF_4$ (76 mg, 0.65 mmol, 1.29 equiv), and $KBAr'_4$ (499 mg, 0.55 mmol, 1.1 equiv) gave an orange-brown low-melting solid (361 mg, 0.28 mmol) by procedure A (95% yield), procedure B (57% yield); ca. 5.2:1 mixture of *exo*/*endo* conformers. Mp: 46−49 °C dec. IR (CH_2Cl_2, KCl, cm^{-1}): 2104 (CO), 1738 (NO). *exo* ^{1}H NMR ($CDCl_3$, 300 MHz): δ 2.87 (dd, $^3J_{3(anti)-2} = 12.5$ Hz, $^2J_{3(anti)-3(syn)} = 3.0$ Hz, 1 H, C(3)−H_{anti}), 4.60 (m, 1 H, C(3)−H_{syn}), 5.28 (d, $^3J_{1(anti)-2} = 14.7$ Hz, 1 H, C(1)−H_{anti}), 5.42 (dd, $^3J_{1(syn)-2} = 7.3$ Hz, $^4J_{1(syn)-3(syn)} = 3.4$ Hz, 1 H, C(1)−H_{syn}), 5.49 (m, 1 H, C(2)−H), 6.22 (app t, $J = 2.0$ Hz, 1 H, Tp), 6.36 (app t, $J = 2.0$ Hz, 1 H, Tp), 6.42 (app t, $J = 2.0$ Hz, 1 H, Tp), 7.29 (d, $J = 2.0$ Hz, 1 H), 7.52 (br s, 4 H, *p*-CH), 7.65 (d, $J = 2.0$ Hz, 1 H, Tp), 7.70 (br s, 9 H, Tp, *o*-CH), 7.81 (d, $J = 2.0$ Hz, 1 H, Tp), 7.89 (d, $J = 2.0$ Hz, 1 H, Tp), 8.06 (d, $J = 2.0$ Hz, 1 H, Tp). ^{13}C NMR ($CDCl_3$, 75.5 MHz): δ 63.2 (C(3)), 107.8 (Tp), 108.0 (Tp), 108.4 (Tp), 110.3 (C(1)), 114.1 (C(2)), 117.5 (br s, *p*-C), 124.5 (q, $J = 272$ Hz, CF_3), 128.9 (q, $J = 31$ Hz, *m*-C), 137.4 (Tp), 138.4 (Tp), 138.6 (Tp), 141.3 (Tp), 145.5 (Tp), 146.8 (Tp), 161.6 (q, 49 Hz, *i*-C), 203.0 (MoCO). *endo* ^{1}H NMR ($CDCl_3$, 300 MHz): δ 3.15 (dd, $^3J_{3(anti)-2} = 12.0$ Hz, $^3J_{3(anti)-3(syn)} = 3.0$ Hz, 1 H, C(3)−H_{anti}), 4.41 (d, $^3J_{1(anti)-2} = 14.6$ Hz, 1 H, C(1)−H_{anti}), 4.60 (m, 1 H, C(3)−H_{syn}), 5.13 (dd, $^3J_{1(syn)-2} = 7.3$ Hz, $^4J_{1(syn)-3(syn)} = 3.0$ Hz, 1 H, C(1)−H_{syn}), 5.99 (m, 1 H, C(2)−H). All Tp signals for the *endo* rotamer were masked by those of the *exo* rotamer. ^{13}C NMR ($CDCl_3$, 75.5 MHz): δ 66.9 (C(3)), 110.5 (C(2)), 116.6 (C(1)), 142.5 (Tp), 144.4 (Tp), 146.2 (Tp), 204.5 (Mo−CO). Anal. Calcd for $C_{45}H_{27}B_2F_{24}N_7O_2Mo$: C, 42.52; H, 2.14; N, 7.71. Found: C, 42.41; H, 2.14; N, 7.80. ^{1}H NOE, **9-*exo***: presaturation of C(3)−H_{syn} (δ 4.60) resulted in enhancement of C(3)−H_{anti} (δ 2.87, 24%), Tp (δ 7.29, 12%), and C(2)−H (δ 5.49, 8%). Presaturation of C(3)−H_{anti} (δ 2.87)

Table 4. Summary of X-ray Crystal Data, Intensity Collection, and Structure Refinement for [TpMo(CO)(NO)(η^3-C_3H_5)][(3,5-$(CF_3)_2C_6H_3)_4$B] (9a)

formula	$C_{54}H_{27}B_2F_{24}MoN_7O_2$
mol wt	1271.3
a,[a] Å	35.324(10)
b, Å	13.025(3)
c, Å	22.063(5)
β, deg	90.06(1)
V, Å^3	10 151(4)
cryst syst	monoclinic
space group	*C*2/*c*
d_{calcd}, g/cm^3	1.664
Z	8
temp, °C	−100
diffractometer	Siemens P4
radiation	Mo Kα (λ = 0.710 73 Å)
abs coeff (μ), mm^{-1}	0.393
cryst size, mm	0.44 × 0.62 × 0.36
scan speed, deg/min in ω	variable, 5−60
scan range, deg	0.6 + (ωKα_1 − ωKα_2)
scan/bkgd ratio	0.5
scan technique	ω
data collected	$-38 \le h \le 14$, $-14 \le k \le 13$, $-23 \le l \le 30$ ($2° \le 2\theta \le 45°$)
abs cor	semiempirical
min and max transmissn	0.6311, 0.6847
system used, structure soln	Siemens SHELXS-86, Patterson
refinement	Siemens SHELXL-93, full-matrix least squares on F^2
no. of rflns collected	7717
no. of indep rflns	4529
no. of obsd rflns ($I > 4\sigma(I)$)	3583
R_{int}, %	4.58
no. of variables	607
goodness of fit[b]	1.07
R1, %	6.59
R1, % (all data)	8.03
weighting scheme	$w^{-1} = \sigma^2(F_o^2) + (0.1231P^c)^2 + 39.0527P$
max and min diff peaks, e/Å^3	0.693, −0.805
largest and mean Δ/σ	0.002, 0.001

[a] Least-squares treatment of 33 centered reflections between 10 and 25° in 2θ. [b] Goodness of fit = $[\sum(w(F_o^2 - F_c^2)^2)/(n - p)]^{1/2}$, where *n* and *p* denote the number of data and parameters, respectively. [c] Where $P = (F_o^2 + 2F_c^2)3$.

resulted in enhancement of C(3)−H_{syn} (δ 4.60, 22%) and C(1)−H_{anti} (δ 5.28, 5%). Presaturation of C(1)−H_{anti} (δ 5.28) resulted in enhancement of C(1)−H_{syn} (δ 5.42, 17%) and C(3)−H_{anti} (δ 2.87, 4%). Presaturation of Tp doublet (δ 7.29) resulted in enhancement of C(3)−H_{syn} (δ 4.60, 24%) and a Tp doublet (δ 7.14, 14%). Presaturation of Tp doublet (δ 7.14) resulted in enhancement of C(3)−H_{anti} (δ 3.15, 10%). Presaturation of C(1)−H_{anti} (δ 4.41) resulted in enhancement of C(1)−H_{syn} (δ 5.13, 20%).

***endo*-[TpMo(CO)(NO)(η^3-C_4H_7)][(3,5-$(CF_3)_2C_6H_3)_4$B] (10).** *exo*-TpMo(CO)$_2$(η^3-C_4H_7) (232 mg, 0.55 mmol, 1.0 equiv), $NOBF_4$ (77 mg, 0.66 mmol, 1.19 equiv), and KBAr′$_4$ (549 mg, 0.61 mmol, 1.1 equiv) gave a brown, low-melting solid (539 mg, 0.42 mmol) by procedure A; 76% yield. Mp: 40−42 °C dec. IR (CH_2Cl_2, KCl, cm^{-1}): 2112 (CO), 2068, 2014, 1731 (NO). ^{1}H NMR ($CDCl_3$, 300 MHz): δ 2.29 (s, 3 H, Me), 3.07 (d, $^2J_{3(anti)-3(syn)}$ = 2.9 Hz, 1 H, C(3)−H_{anti}), 4.12 (d, $^2J_{1(anti)-1(syn)}$ = 1.5 Hz, 1 H, C(1)−H_{anti}), 4.39 (dd, $^4J_{3(syn)-1(syn)}$ = 4.4 Hz, $^2J_{3(anti)-3(syn)}$ = 2.9 Hz, 1 H, C(3)−H_{syn}), 4.80 (br d, $^4J_{1(anti)-3(syn)}$ = 4.0 Hz, 1 H, C(1)−H_{syn}), 6.26 (app t, *J* = 2.0 Hz, 1 H, Tp), 6.42 (app t, *J* = 2.0 Hz, 1 H, Tp), 6.45 (app t, *J* = 2.0 Hz, 1 H, Tp), 7.22 (d, *J* = 2.0 Hz, 1 H, Tp), 7.51 (br s, 4 H, *p*-CH), 7.68 (br s, 9 H, *o*-CH, Tp), 7.77 (d, *J* = 2.0 Hz, 1 H, Tp), 7.82 (m, 2 H, Tp), 7.86 (d, *J* = 2.0 Hz, 1 H, Tp). ^{13}C NMR ($CDCl_3$, 75.5 MHz): δ 22.7 (Me), 68.0 (C(3)), 104.7 (C(1)), 107.9 (Tp), 108.2 (Tp), 117.6 (q, *J* = 272 Hz, *p*-C), 124.5 (q, *J* = 29 Hz, CF_3), 129.0 (br s, *m*-C), 134.0 (C(2)), 134.8 (br s, *o*-C), 138.4 (Tp), 139.0 (Tp), 142.1 (Tp), 144.5 (Tp), 145.9 (Tp), 161.7 (q, *J* = 50 Hz, *i*-C), 201.9 (Mo−CO). Anal. Calcd for $C_{46}H_{29}B_2F_{24}N_7O_2$Mo: C, 42.99; H, 2.27; N, 7.63. Found: C, 42.76; H, 2.31; N, 7.56. ^{1}H NOE for **10**: presaturation of C(3)−H_{anti} (δ 3.07) resulted in enhancement of a Tp doublet (δ 7.22, 18%), C(3)−H_{syn} (δ 4.39, 21%), and C(1)−H_{anti} (δ 4.12, 5%); presaturation of C(1)−H_{anti} (δ 4.12) resulted in enhancement of C(1)−H_{syn} (δ 4.80, 20%); presaturation of Tp doublet (δ 7.22) resulted in enhancement of C(3)−H_{anti} (δ 3.07, 14%).

***exo*-[TpMo(CO)(NO)(η^3-C_6H_9)][(3,5-$(CF_3)_2C_6H_3)_4$B] (11).** *exo*-TpMo(CO)$_2$(η^3-C_6H_9) (296 mg, 0.66 mmol, 1.0 equiv), $NOBF_4$ (101 mg, 0.86 mmol, 1.30 equiv), and KBAr′$_4$ (659 mg, 0.73 mmol, 1.1 equiv) gave an orange-brown solid (771 mg, 0.59 mmol) by procedure A; 89% yield. Mp: 75−79 °C dec. IR (CH_2Cl_2, KCl, cm^{-1}): 2079 (CO), 1725 (NO). ^{1}H NMR ($CDCl_3$, 300 MHz): δ 1.34 (m, 1 H, CH_2), 1.53 (m, 1 H, CH_2), 2.35 (m, 1 H, CH_2), 2.99 (m, 3 H, CH_2), 5.30 (m, 2 H, C(2)−C(3)−H), 6.25 (app t, *J* = 2.0 Hz, 1 H, Tp), 6.32 (app t, *J* = 2.0 Hz, 1 H, Tp), 6.41 (app t, *J* = 2.0 Hz, 1 H, Tp), 7.16 (m, 1 H, C(1)−H_{syn}), 7.44 (d, *J* = 3.0 Hz, 1 H, Tp), 7.51 (br s, 4 H, *p*-CH), 7.71 (br s, 11 H, Tp, *p*-CH), 7.81 (d, *J* = 3.0 Hz, 1 H, Tp), 8.09 (d, *J* = 2.0 Hz, 1 H, Tp). ^{13}C NMR ($CDCl_3$, 75.5 MHz): δ 17.4 (CH_2), 25.2 (CH_2), 26.1 (CH_2), 79.0 (C(3)), 98.8 C(2)), 107.7 (Tp), 108.1 (Tp), 117.4 (br s, *p*-C), 120.9 (q, *J* = 272 Hz, CF_3), 129.0 (q, *J* = 29 Hz, *m*-C), 134.7 (br s, *o*-C), 136.9 (Tp), 138.4 (Tp), 138.5 (Tp), 141.0 (Tp), 145.4 (Tp), 145.8 (Tp), 149.1 (C(1)), 161.6 (q, *J* = 50 Hz, *i*-C), 206.3 (Mo−CO). Anal. Calcd for $C_{48}H_{31}B_2F_{24}N_7O_2$Mo: C, 43.96; H, 2.38; N, 7.48. Found: C, 44.03; H, 2.37; N, 7.47. ^{1}H NOE for **11**: presaturation of C(1)−H (δ 7.16) resulted in enhancement of a Tp doublet (δ 7.81, 18%) and C(2)−H (δ 5.30, 9%); presaturation of Tp signal (δ 7.45) resulted in enhancement of C(2),C(3)−H (δ 5.30, 19%); presaturation of C(2),C(3)−H (δ 5.30) resulted in enhancement of a Tp doublet (δ 7.45, 15%).

***exo*-[TpMo(CO)(NO)(η^3-C_8H_{13})][(3,5-$(CF_3)_2C_6H_3)_4$B] (12).** *exo*-TpMo(CO)$_2$(η^3-C_8H_{13}) (267 mg, 0.56 mmol, 1.0 equiv), $NOBF_4$ (66 mg, 0.56 mmol, 1.0 equiv), and KBAr′$_4$ (509 mg, 0.56 mmol, 1.0 equiv) gave a brown solid (680 mg, 0.58 mmol) by procedure B; 90% yield. Mp: 78−80 °C dec. (CH_2Cl_2/hexane, 1:4). IR (CH_2Cl_2, KCl, cm^{-1}): 2519 (BH), 2079 (CO), 1717 (NO). ^{1}H NMR ($CDCl_3$, 300 MHz): δ 1.74 (m, 6 H), 1.95 (m, 1 H), 2.73 (m, 2 H), 3.09 (m, 1 H), 5.24 (app q, ^3J = 8.1 Hz, 1 H, C(3)−H_{syn}), 5.32 (app t, *J* = 8.1 Hz, 1 H, C(2)−H), 6.22 (app t, *J* = 2.2 Hz, 1 H), 6.36 (app t, *J* = 2.2 Hz, 1 H), 6.42 (app t, *J* = 2.2 Hz, 1 H), 6.74 (app q, ^3J = 8.1 Hz, 1H, C(1)−H_{syn}), 7.36 (d, *J* = 3.0 Hz, 1 H), 7.51 (br s, 4 H), 7.65 (d, *J* = 3.0 Hz, 1 H), 7.70 (br s, 8 H), 7.72 (m, 2 H), 7.93 (d, *J* = 2.2 Hz, 1 H), 8.05 (d, *J* = 2.2 Hz, 1 H). ^{13}C NMR ($CDCl_3$, 75.5 MHz): δ 22.4 (CH_2), 26.3 (CH_2), 27.5 (CH_2), 29.6 (CH_2), 31.8 (CH_2), 83.1 (C(3)), 106.7 (C(2)), 107.7 (Tp), 107.8 (Tp), 108.1 (Tp), 117.5 (*p*-C), 124.5 (q, *J* = 272 Hz, CF_3), 128.8 (q, *J* = 29.3, *m*-C), 134.8 (br s, *o*-C), 137.1 (Tp), 138.3 (Tp), 138.4 (Tp), 141.0 (Tp), 145.4 (Tp), 146.4 (Tp), 147.5 (C(1)), 161.6 (q, *J* = 50 Hz, *i*-C), 206.6 (CO). Anal. Calcd for $C_{50}H_{35}B_2F_{24}N_7O_2$Mo: C, 44.84; H, 2.63; N, 7.32. Found: C, 45.20; H, 3.05; N, 7.01. ^{1}H NOE for **12**: presaturation of C(1)−H (δ 6.76) resulted in enhancement of a Tp signal (δ 7.93, 7%); presaturation of C(3)-H (δ 5.24) resulted in enhancement of a Tp signal (δ 7.36, 10.5%).

X-ray Crystal Structure Determination of [TpMo(CO)(NO)(η^3-C_3H_5)][(3,5-$(CF_3)_2C_6H_3)_4$B] (9a). A fragment of dimensions 0.44 × 0.62 × 0.36 mm was cut from a large rhombic yellow crystal, mounted under oil on a quartz fiber with cyanoacrylate glue, and placed in a cold stream at −100 °C (provided by an LT-2 low-temperature delivery system) on a Siemens P4 diffractometer for data collection. The orientation matrices and unit cell parameters were determined by least-squares treatment of 33 centered reflections between 10 and 25° in 2θ. Crystal data, reflection intensity collection parameters, and structure refinement data are provided in Table 4. The intensities of three check reflections (4,−2,2, 5,1,−1, 323 monitored every 100 reflections at approximately 1 h intervals) exhibited little decay. A semiempirical correc-

tion for absorption, using azimuthal ψ scans, was applied, and all data were corrected for *Lp* effects.

The structure was solved by the Patterson method and refined by full-matrix least squares using the program SHELXL-93 (Siemens Analytical X-ray instruments, Inc., Madison, WI). The hydrogen atoms were included, but not refined in calculated positions (C−H = 0.96 Å) with isotropic thermal parameters set at 0.05 times that of the parent atom. All non-hydrogen atoms of the cation were refined with anisotropic thermal parameters. The non-hydrogen atoms of the anion were also refined with anisotropic thermal parameters, except the aromatic ring carbons, which were refined isotropically to reduce the number of least-squares parameters and a disordered $-CF_3$ which was modeled and also refined isotropically. The maximum shift/ESD for the final cycle was 0.002, and the maximum and minimum peaks in the difference electron density map were +0.693 and −0.805 e/Å^3. Least-squares refinement converged to the *R* factors provided in Table 4. Tables of atom coordinates are shown in Table 5 (Supporting Information). Complete bond lengths and bond angles for the cation of **9a** are shown in Table S-1, thermal parameters in Table S-2, and hydrogen fixed positional parameters and temperature factors in Table S-3 can be found in the Supporting Information.

Acknowledgment. This investigation was supported by Grant No. GM 43107, awarded by the National Cancer Institute, DHHS. We acknowledge the use of a VG-mass spectrometer purchased through funding from the National Institutes of Health (Grant No. S10-RR-02478) and a 300 MHz NMR and 360 MHz NMR purchased through funding from the National Science Foundation (Grant No. NSF CHE-85-16614 and NSF CHE-8206103, respectively). We acknowledge Dr. Shaoxiong Wu, Danita Kiser, and Scott Moore for assistance with the HETCOR, NOESY, and COSY experiments. L.A.V. acknowledges funding from the NIH through a minority supplement to Grant No. GM 43107.

Supporting Information Available: An ORTEP drawing and tables giving all bond lengths and bond angles, hydrogen fixed positional parameters and temperature factors, thermal parameters, and positional parameters for non-hydrogen atoms (11 pages). Ordering information is given on any current masthead page.

OM960041X